RSC Advances

PAPER

View Article Online
View Journal | View Issue

Cite this: *RSC Adv.*, 2021, **11**, 12826

Effects of alternating current poling on the dielectric and piezoelectric properties of $Pb(In_{0.5}Nb_{0.5})O_3$–$PbTiO_3$ crystals with a high Curie temperature

Junjie Xiong,[abc] Zujian Wang,[a] Xiaoming Yang,[a] Rongbing Su,[a] Xifa Long *[abc] and Chao He *[abc]

Received 4th December 2020
Accepted 21st March 2021

DOI: 10.1039/d0ra10234b

rsc.li/rsc-advances

The alternating current poling (ACP) method has been become more and more popular recently because of its advantages of being low cost, time saving and highly efficient. Few ACP studies have focused on relaxor-PT crystals with a high coercive field and high Curie temperature or the effects of ACP on intrinsic and extrinsic contributions. The effects of the electric field, frequency, and number of cycles of ACP on the piezoelectric and dielectric properties of ⟨001⟩-oriented $Pb(In_{0.5}Nb_{0.5})O_3$–$PbTiO_3$ ferroelectric crystals were studied. The dielectric permittivity $\varepsilon_{33}^T/\varepsilon_0$ and piezoelectric coefficient d_{33} of an ACP sample are 3070 and 1400 pC N^{-1}, respectively, which are 14% and 18% larger than those of a DCP sample. Rayleigh analysis reveals that both intrinsic and extrinsic contributions are enhanced after ACP. The poling electric field, frequency and cycle number can influence the intrinsic and extrinsic contributions. The intrinsic contribution is significantly affected by the poling electric field, and cycle number, but it is not very sensitive to frequency, while the poling electric field, frequency and cycle number are very important for the extrinsic contribution. This work demonstrates that the uniform domain patterns are a critical factor for the enhancement of the piezoelectric properties.

1. Introduction

Relaxor-$PbTiO_3$ (relaxor-PT) ferroelectric crystals, such as $Pb(Mg_{1/3}Nb_{2/3})O_3$–$PbTiO_3$ (PMN–PT), have been widely used in sensors, actuators, and transducers, owing to their outstanding piezoelectric coefficient (d_{33}) and high electromechanical coupling factor (k_{33}) ($d_{33} > 2000$ pC N^{-1}, $k_{33} > 0.9$).[1–3] Although rhombohedral PMN–PT crystals a have ultrahigh piezoelectric performance, its low Curie temperature ($T_C \sim 150$ °C) and small coercive field ($E_c = 2$–3 kV cm^{-1}) restrict its applications at high temperature and high power. $Pb(In_{0.5}Nb_{0.5})O_3$–$PbTiO_3$ (PIN–PT) crystals exhibit a high T_C (>250 °C) and large E_c (~8 kV cm^{-1}), which can fill the demands at a high temperature and high field.[4,5] The piezoelectric properties of PIN–PT crystals ($d_{33} \sim$ 1500 pC N^{-1}, $k_{33} \sim 85\%$) are not as excellent as those of the PMN–PT crystals. How to promote the piezoelectricity of PIN–PT crystals is a good issue for broader device applications.

In recent years, many methods have been introduced to further enhance the piezoelectric properties of relaxor-PT crystals. These strategies include adjusting the compositions, doping, using nano-electrodes, choosing better poling conditions and so on.[6–19] For instance, recent studies found that Sm doped in a PMN–PT system can significantly improve the piezoelectricity.[14,17] Davis *et al.* presented how to choose the optimal direction for poling to get a high piezoelectric performance.[16] Design of the morphotropic phase boundary (MPB) can also get an excellent piezoelectric performance due to the flattened free-energy profile.[18,19] A decrease of the domain size is on additional effective way to promote the piezoelectricity.[10,11]

Among the above methods, alternating current field poling (ACP) became more and more popular recently because of its advantages of low-cost, time-saving and high-efficiency. It has been reported that ACP is a highly efficient technique to get a high piezoelectric performance of PMN–PT crystals and can make a 40% enhancement of d_{33},[20] while the mechanisms of the ACP method are not clear enough. Many scientists put forward their ideas on the mechanisms of ACP. Chang *et al.* proposed that the reason for the excellent piezoelectric performance originates from the monoclinic phase (M_A).[21] Luo *et al.* used domain growth theory to explain the transformation process of the domain structure.[22] Qiu *et al.* presented a new idea that the improvement of the piezoelectric performance originates from polar nano regions (PNRs) or the local structure.[23] He *et al.* subsequently investigated the $Pb(Yb_{0.5}Nb_{0.5})O_3$–PMN–PT

[a]*Key Laboratory of Optoelectronic Materials Chemistry and Physics, Fujian Institute of Research on the Structure of Matter, Chinese Academy of Sciences, Fuzhou, 350002, China. E-mail: hechao@fjirsm.ac.cn; lxf@fjirsm.ac.cn*

[b]*Fujian Science & Technology Innovation Laboratory for Optoelectronic Information of China, Fuzhou, 350108, China*

[c]*University of Chinese Academy of Sciences, Beijing, 100049, China*

system, and concluded that a highly ordered domain structure results in a high piezoelectric performance after ACP.[8] Qiu *et al.* proposed that the enhancement of piezoelectric performance is related to the decrement of the 71° domain wall.[24] To summarize, ACP has become a promising poling method compared with the traditional direct current poling (DCP) method, but the mechanisms is still a big challenge. At present, most of the reported ACP studies have focused on relaxor-PT crystals with a low E_c, such as PMN–PT and PIN–PMN–PT, while little attentions is paid to relaxor-PT crystals with a high T_C and large E_c. In addition, the enhancement of the piezoelectric properties after ACP are related to a change of domain configuration. It is generally said that the contributions of the domain wall motion are thought to be an extrinsic contribution, which is unclear.

In this work, the piezoelectric and dielectric properties of PIN–PT crystals with a large E_c and high T_C were studied using different poling electric fields, frequencies, and cycles of ACP. The Rayleigh analysis and domain structure were studied to track the relationship between the enhancement of piezoelectric properties and domain engineering.

2. Experimental procedure

The rhombohedral perovskite phase PIN–PT crystals with an E_c of 8.6 kV cm^{-1} and T_C of 260 °C were grown in our lab using a top-seeded solution growth method. The details of the growth have been reported in our previous work.[5] The actual composition was 0.66PIN–0.34PT examined by inductively coupled plasma atomic emission spectroscopy (ICP-AES, JY Ultima-2, Horiba Jobin Yvon, France). The natural {001} face can be obtained from as-grown crystals, and was examined using XRD. Then, crystals were cut into ⟨001⟩-oriented samples: dimensions of 4 × 4 × 0.6 mm^3 (plate mode) were used for the dielectric and piezoelectric measurements and of 5 × 1 × 1 mm^3 (bar mode) for the electromechanical coupling factor measurements. The grown PIN–PT crystals exhibit a natural {001} face. The {001} crystal plates were cut parallel to the natural {001} face. And the cut crystal plates were examined using XRD. All the samples were annealed at 600 °C for 6 h, with the top and bottom electrodes shorted to eliminate the residual stress fully before each poling measurement.

In this work, a high-voltage supply amplifier/controller (Trek, model 610E) was used for DCP and ACP. The voltage presented in this work for DCP is a peak voltage (V_{peak}), while the voltage presented in this work for ACP is a root mean square voltage (V_{rms}) of the triangle voltage (Fig. 1b). The poling processes were carried out at ambient temperature in silicon oil to protect the samples. d_{33} of PIN–PT single crystals was measured using a quasi-static d_{33} meter (Chinese Academy of Sciences, Institute of Acoustics, ZJ-4AN, China). The free dielectric constant ($\varepsilon_{33}{}^T/\varepsilon_0$) were measured by an impedance analyzer (Keysight Technologies, E4990A, Santa Clara, CA, USA). k_{33} was calculated from the resonance frequency (f_r) and anti-resonance frequency (f_a) according to IEEE standards. Piezo-response force microscopy (PFM, Asylum Research, Cypher ES, USA) was used to study the domain structure.

3. Results and discussion

3.1 Poling conditions

In the ACP process, the poling electric field, frequency and cycles can affect the piezoelectric performance and interact. The most important factor among the three is the electric field. Therefore, the influence of the electric field was firstly investigated in this work. In the process, the frequency and cycle were the fixed values (frequency: 10 Hz, cycle: 25), which refers to our experience and previous studies in PMN–PT and PIN–PMN–PT crystals. The influence of cycles was studied last because the cycles depend more on the electric field and frequency compared with other factors.

Fig. 1 shows the d_{33}, $\varepsilon_{33}{}^T/\varepsilon_0$ and k_{33} of 0.66PIN–0.34PT crystals after DCP and ACP (10 Hz, 25 cycles) as a function of the electric field. The d_{33} and $\varepsilon_{33}{}^T/\varepsilon_0$ of the DCP samples increased significantly from 790 pC N^{-1} to 1180 pC N^{-1}, and 1950 to 2690, respectively, when the poling electric field increased from 8 to 12 kV cm^{-1}. The d_{33} of the DCP samples decreased when the electric field increased above 16 kV cm^{-1}. The optimal DCP conditions were 12–16 kV cm^{-1} (15 minutes). For the ACP samples, the maximum d_{33}, $\varepsilon_{33}{}^T/\varepsilon_0$ and k_{33} were 1320 pC N^{-1}, 2950 and 85%, respectively, at an electric field of 11.6 kV cm^{-1}, which was 11.9%, 9.7% and −2% higher than that of the DCP samples. Therefore, the optimal ACP root mean square electric field was 11.6 kV cm^{-1}. Note that the variation of d_{33}, $\varepsilon_{33}{}^T/\varepsilon_0$ and k_{33} had a decreasing trend when the electric fields were too large. The electrostrictive effect is generated in the poling process because of the rotation of domains. The crystals are prone to micro-cracking if the poling electric field is too large, which is considered as an over-poling effect.[25–27]

Fig. 2 shows the d_{33}, $\varepsilon_{33}{}^T/\varepsilon_0$ and k_{33} of 0.66PIN–0.34PT crystals after DCP and ACP (11.6 kV cm^{-1}, 25 cycles) as a function of frequency. The values of d_{33} and $\varepsilon_{33}{}^T/\varepsilon_0$ increased dramatically from 1140 pC N^{-1} to 1400 pC N^{-1}, and from 2620 to 3070, respectively when the poling frequency increased from 1 to 15 Hz. Further increasing the poling frequency, the d_{33}, $\varepsilon_{33}{}^T/\varepsilon_0$ gradually decreased. The values of d_{33} and $\varepsilon_{33}{}^T/\varepsilon_0$ were 970 pC N^{-1} and 2150 using 40 Hz poling. For the k_{33}-mode sample, the value of k_{33} of the 0.66PIN–0.34PT crystals decreased with increasing frequencies (Fig. 2b). The highest k_{33} was 86% at 1 Hz. The difference between the variation of k_{33} and d_{33} is related to the shape of the samples. The thickness of the k_{33} mode (5 mm) was much larger than that of the d_{33} sample (0.6 mm), which indicates that the frequency has a relatively large impact on the different thickness samples.[28] Considering both the effect of the frequency on d_{33} and k_{33}, the optimal poling frequency was 15 Hz. Compared with PMN–PT crystals, the piezoelectric and dielectric properties of 0.66PIN–0.34PT crystals after ACP are more dependent on frequency. The previous work revealed that the piezoelectric performances of PMN–PT and PIN–PMN–PT crystals can be significantly improved using low frequency ACP,[29,30] while low frequency ACP does not show any good results for PIN–PT crystals. For PIN–PT crystals, it is hard to switch domains under and external field due its high coercive field. At a low frequency ACP, the domains can easily

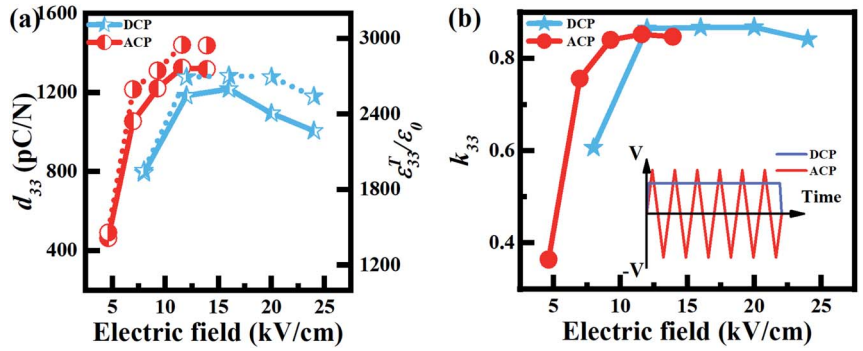

Fig. 1 The (a) d_{33}, $\varepsilon_{33}{}^T/\varepsilon_0$, and (b) k_{33} values of DCP and ACP (10 Hz, 25 cycles) 0.66PIN–0.34PT single crystals as a function of the electric field.

grow large, which further hinders domain switching. It is detrimental to rearrange domains and enhance the performance.

Fig. 3 shows the d_{33}, $\varepsilon_{33}{}^T/\varepsilon_0$ and k_{33} of 0.66PIN–0.34PT crystals after DCP and ACP (15 Hz, 11.6 kV cm^{-1}) as a function of cycle. The values of d_{33}, $\varepsilon_{33}{}^T/\varepsilon_0$ and k_{33} increased significantly from 690 pC N^{-1}, 1660 and 66% to 1400 pC N^{-1}, 3070 and 86%, respectively, when the ACP cycle increased from 5 to 25, and became invariant with a further increase of the ACP cycle. The optimal poling cycle was 25. The reported PMN–PT single crystals have the highest piezoelectric properties with poling cycles below 10.[22] The ACP process can reduce the energy required for domain rotation, which makes domain rotation easy.[28] The poling cycle is the process of the reduction of the energy required for domain rotation. Compared with PMN–PT crystals, the PIN–PT crystal required more energy for domain rotation due to its higher coercive field. Therefore, PIN–PT crystals need more poling cycles to obtain the maximum piezoelectric coefficient compared to those for PMN–PT crystals.

Based on the above results, the d_{33} and $\varepsilon_{33}{}^T/\varepsilon_0$ of 0.66PIN–0.34PT crystals can be enhanced using ACP. The optimal ACP conditions were 11.6 kV cm^{-1}, 15 Hz and 25 cycles. Under these poling conditions, the d_{33}, $\varepsilon_{33}{}^T/\varepsilon_0$ and k_{33} of 0.66PIN–0.34PT crystals can achieve values of 1400 pC N^{-1}, 3070, and 86%, respectively. Table 1 shows a comparison of the piezoelectric and dielectric properties of relaxor-PT crystals.[8,21,22,31,32] Compared with relaxor-PT crystals with a low E_c (<6 kV cm^{-1}), the enhancement ratio of ACP 0.66PIN–0.34PT crystals is not as high as for these crystals. Polarization switching can reflect the domain wall motions and opposite domain nucleation and growth in the ACP process.[33] The PMN–PT crystals have a fast domain nucleation and growth due to their low coercive field.[22] It is difficult to rearrange the domain structure of 0.66PIN–0.34PT crystals due to the large coercive field, resulting in the small enhancement after ACP.

3.2 Rayleigh analysis

The enhancement of piezoelectric and dielectric properties can be divided into the enhancement of intrinsic and extrinsic contributions. The intrinsic contribution originates from lattice distortion, while the extrinsic contribution originates from the domain wall and phase boundary motion. The degrees of intrinsic and extrinsic contributions can be well-distinguished by the Rayleigh law.[34–37] the Rayleigh law can be expressed using the following formulas:[38,39]

$$P(E) = \varepsilon_0(\varepsilon_{\text{init}} + \alpha E_0)E \pm \alpha({E_0}^2 - E^2)/2 \quad (1)$$

$$\varepsilon_r = \varepsilon_{\text{init}} + \alpha E_0 \quad (2)$$

where P is the polarization, and E_0 is the amplitude of the measured AC field, ε_r is the total dielectric permittivity under the electric field. $\varepsilon_{\text{init}}$ is ε_r when the limit E_0 tends to 0 and represents the reversible part, which consists of the intrinsic

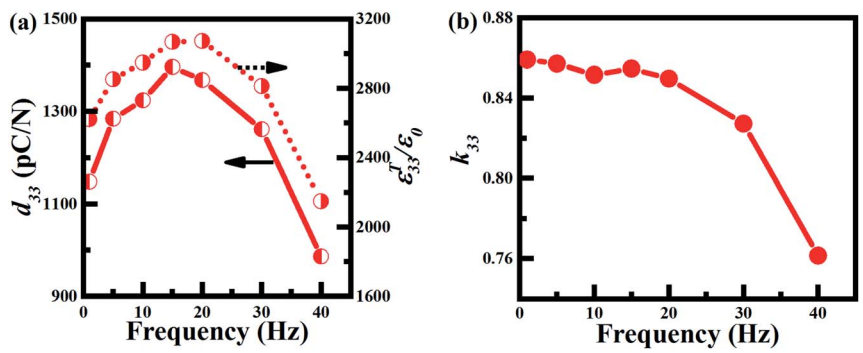

Fig. 2 The d_{33}, $\varepsilon_{33}{}^T/\varepsilon_0$, and k_{33} values of ACP (11.6 kV cm^{-1}, 25 cycles) 0.66PIN–0.34PT crystals as a function of frequency.

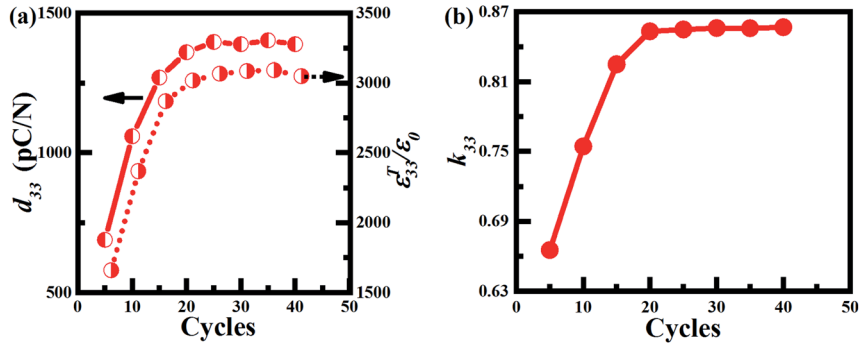

Fig. 3 The d_{33}, $\varepsilon_{33}{}^T/\varepsilon_0$, and k_{33} values of ACP (15 Hz, 11.6 kV cm^{-1}) 0.66PIN–0.34PT crystals as a function of the poling cycle number.

contribution and the reversible domain wall motion. For most relaxor-PT ferroelectrics, the intrinsic contributions play the dominant role in the reversible part, while the proportion of the reversible domain wall motion is small.[40,41] Thus, ε_{init} is approximate to the intrinsic contribution of dielectric permittivity and αE_0 is the extrinsic contribution of dielectric permittivity; α is the Rayleigh coefficient that represents the contribution of the domain wall motion and phase boundary. The ratio of the extrinsic contribution is expressed as:

$$\text{Extrinsic ratio} = \alpha E_0/(\varepsilon_{init} + \alpha E_0) \quad (3)$$

Eqn (1) describes the Rayleigh hysteresis, where the signs "+" and "−" correspond to decreasing and increasing electric field, respectively. To avoid the switching of domains, E_0 is selected far lower than half of the E_c. In this work, the E_0 was 1–3 kV cm^{-1} and the extrinsic ratio was calculated at E_0 of 1 kV cm^{-1}. From the slope of the *P*–*E* at a low electric field, the value of $\varepsilon_{init} + \alpha E_0$ can be expressed as:

$$\varepsilon_r = \varepsilon_{init} + \alpha E_0 = (P_{max} - P_{min})/2(E_0\varepsilon_0) \quad (4)$$

where P_{max} and P_{min} are the largest and lowest value of polarization in the *P*–*E* hysteresis loops.

Fig. 4 shows the Rayleigh analysis of the 0.66PIN–0.34PT crystals under different electric fields. It can be easily obtained that the value of ε_r is linear with E_0, suggesting that the Rayleigh law is applicable for 0.66PIN–0.34PT crystals with E_0 from 1 to 3 kV cm^{-1}. According to eqn (2), the intercept from the *y* axis represents ε_{init} and the slope of the lines represents α. Hence, the values of ε_{init} and αE_0 were found to be 2788 and 209, respectively, for the DCP samples. The value of ε_{init} was 2286 for the ACP samples under 6.96 kV cm^{-1}, which was much smaller than that for the DCP samples. Further increasing the ACP electric field from 6.96 kV cm^{-1} to 11.6 kV cm^{-1}, the values of ε_{init} and αE_0 all increased dramatically from 2286 and 214 to 2875 and 327, respectively, indicating that both the intrinsic and extrinsic contributions enhanced after ACP. The increment of the ratio of $\alpha E_0/(\varepsilon_{init} + \alpha E_0)$ indicates the obvious enhancement of the extrinsic contribution. The highest value of $\alpha E_0/(\varepsilon_{init} + \alpha E_0)$ was 0.102 at the poling electric field of 11.6 kV cm^{-1}. It can be concluded that the extrinsic contribution is affected heavily by the ACP.

Fig. 5 shows the Rayleigh analysis of 0.66PIN–0.34PT ACP samples under different poling frequencies. With the increase of the frequency from 1 Hz to 15 Hz, the intrinsic contribution ε_{init} increased slightly from 2760 to 2919, while the extrinsic contribution αE_0 exhibited a great improvement from 226 to 351, and the proportion of $\alpha E_0/(\varepsilon_{init} + \alpha E_0)$ increased significantly from 0.076 to 0.107. When the frequency exceeded 15 Hz, the values of ε_{init} and αE_0 began to decline. The values of ε_{init} and αE_0 were 2043 and 280, respectively, at 40 Hz, which were much smaller than those at 15 Hz. It can be concluded that a low ACP frequency has little effect on the intrinsic contribution. When the ACP frequency was high, both the intrinsic and extrinsic contributions declined significantly. Therefore, ACP of a moderate frequency is critical and necessary, such as 15 Hz in this work.

Fig. 6 shows the Rayleigh analysis of 0.66PIN–0.34PT ACP samples under different poling cycles. When the cycles increased from 5 to 25, the intrinsic contribution ε_{init} and the

Table 1 Dielectric and piezoelectric properties of relaxor-PT crystals after DCP and ACP. T_{rt}: rhombohedral–tetragonal phase transition temperature

Material	E_c (kV cm^{-1})	T_{rt} (°C)	T_C (°C)	$\varepsilon_{33}{}^T/\varepsilon_0$ DCP	$\varepsilon_{33}{}^T/\varepsilon_0$ ACP	d_{33} (pC N^{-1}) DCP	d_{33} (pC N^{-1}) ACP	Difference (d_{33})	Ref.
0.52PMN–0.15PYbN–0.33PT	5.4	94	180	5200	6800	1770	2490	41%	8
0.75PMN–0.25PT	2.6	93	116	—	6397	1220	1730	42%	22
0.7PMN–0.3PT	2.3	90	130	6120	8140	1650	1980	20%	21
0.72PMN–0.28PT	—	80	132	7000	8900	1940	2650	37%	31
0.25PIN–0.43PMN–0.32PT	—	113	180	4800	7120	1700	2610	54%	32
0.66PIN–0.34PT	8.6	160	260	2690	3070	1180	1400	18%	This work

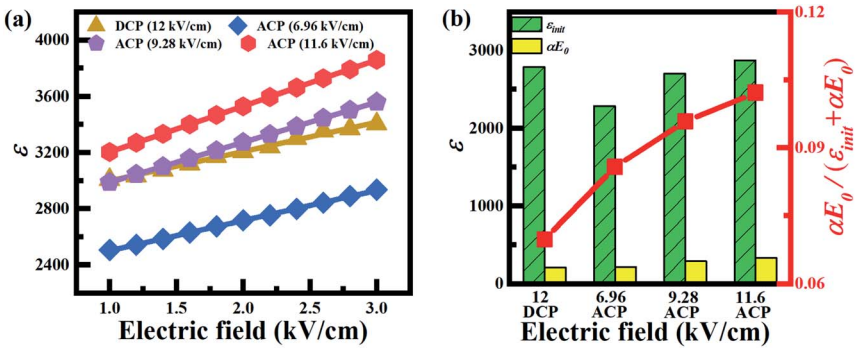

Fig. 4 The Rayleigh analysis of DCP and ACP (10 Hz, 25 cycles) samples under different electric fields.

extrinsic contribution αE_0, and the proportion of $\alpha E_0/(\varepsilon_{init} + \alpha E_0)$, increased from 1787, 152, 0.078 to 2919, 351 and 0.107, respectively. Then, the values of ε_{init}, αE_0, and $\alpha E_0/(\varepsilon_{init} + \alpha E_0)$ all became invariant when the cycles exceeded 25, indicating that the optimal poling cycle was 25 cycles.

The poling electric field, frequencies and cycles can influence the intrinsic and extrinsic parts of the ACP samples. The intrinsic contribution is significantly affected by the poling electric field and cycle, but it is not very sensitive to frequency, while the poling electric field, frequency and cycle is very important for the extrinsic contribution. The values of ε_{init}, αE_0 and $\alpha E_0/(\varepsilon_{init} + \alpha E_0)$ were 2919, 351 and 0.107, respectively, with an electric field of 11.6 kV cm^{-1}, frequency of 15 Hz, and 25 cycles.

3.3 Domain structures

The enhancement of the piezoelectric and dielectric properties after ACP are related to the optimization of the domain morphologies.[8,21,22,24] It should also be noted that 0.66PIN–0.34PT crystals have the rhombohedral perovskite phase. The ferroelectric crystals with the rhombohedral perovskite phase have eight spontaneous directions along ⟨111⟩. Poling along the ⟨001⟩ direction, the "4R" domain-engineered multi-domain structure is formed, exhibiting clear 109° and 71° domain walls.

Fig. 7 shows the PFM results of the unpoled, DCP and ACP samples. The scan area is 20 × 20 μm^2 for each image. The crystallographic orientation and poling direction are marked in Fig. 7. For the unpoled sample, PIN–PT crystals exhibit a clear domain boundary and the strip domain is aligned along the diagonal orientation. It is difficult to distinguish the 109° and 71° domains. The 109° and 71° domain walls can be easily distinguished due to the formation of the typical '4R' domain configuration after poling. For DCP samples, the domain boundary between the 109° and 71° domain walls may form an irregular and overlapping domain structure. For ACP samples (11.6 kV cm^{-1}, 15 Hz, 25 cycles), the 71° domain walls degrade and the 109° domain walls became clear and stable. The 109° domain walls tend to be perpendicular to the electric field direction and form regular stripe-like layered structures after ACP. The same results have also been confirmed in our previous work.[8]

The previous reported deemed that the high piezoelectricity was attributed to the high domain wall density of 71° domain walls.[21] Different from those high-density 71° domain walls in ACP relaxor-PT single crystals, 0.66PIN–0.34PT crystals have a high density of regular 109° domain walls and a low density of 71° domain walls, which is closer to the simulations in PMN–PT systems.[24] Therefore, the uniform and stripe like 109° domain wall patterns are a critical factor for the enhancement of piezoelectric properties *via* domain engineering.

4. Conclusions

The effects of ACP on 0.66PIN–0.34PT crystals were studied, including changing the electric field, frequency, and cycle

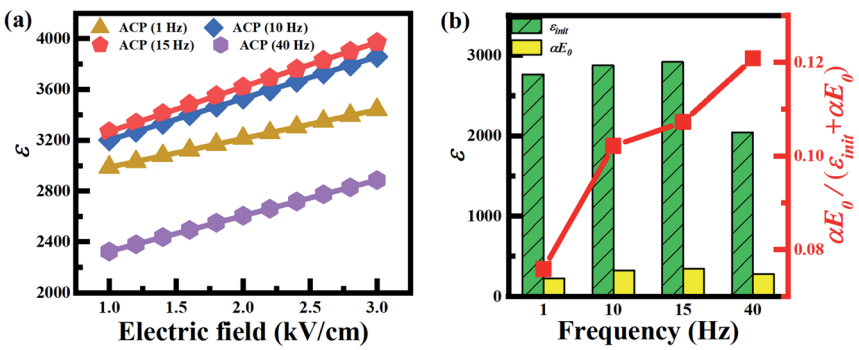

Fig. 5 The Rayleigh analysis of ACP samples under different poling frequencies (11.6 kV cm^{-1}, 25 cycles).

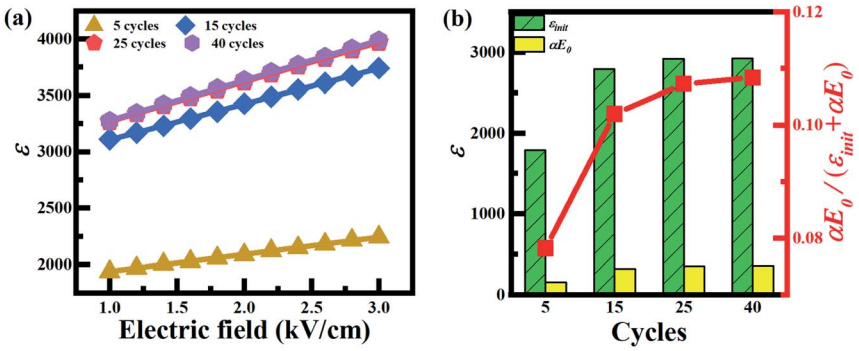

Fig. 6 The Rayleigh analysis of ACP samples with different poling cycle numbers (15 Hz, 11.6 kV cm^{-1}).

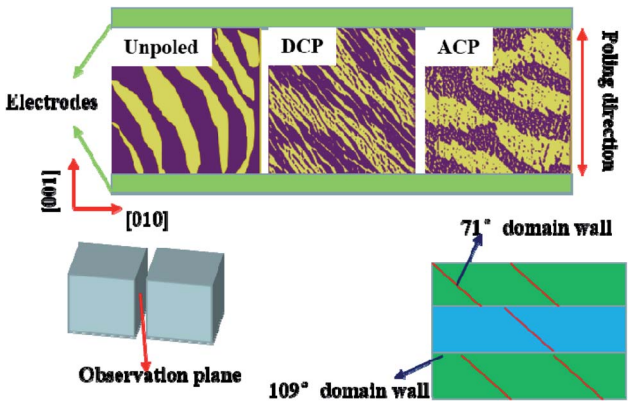

Fig. 7 The domain structures of unpoled, DCP and ACP samples (all scan areas are 20 × 20 μm^2).

number. The optimal ACP conditions are an electric field of 11.6 kV cm^{-1}, a poling frequency of 15 Hz, and a cycle number of 25. The $\varepsilon_{33}{}^{T}/\varepsilon_0$ and d_{33} values were 3070 and 1400 pC N^{-1}, respectively, after ACP, which were about 14% and 18%, respectively, better than those of conventional DCP samples, while the k_{33} values of both DCP and ACP 0.66PIN–0.34PT crystals had the same level. Rayleigh analysis revealed that both the intrinsic and extrinsic contributions were enhanced after ACP. The poling electric field, frequency, and cycle number can influence the intrinsic and extrinsic contributions. The highly regular, uniform domain structure of the 109° domains and low density of the 71° domains were the obvious differences between unpoled, ACP, and DCP samples. The uniform and stripe like 109° domain wall patterns are a critical factor for the enhancement of the piezoelectric properties *via* domain engineering.

Conflicts of interest

There are no conflicts to declare.

Acknowledgements

This work was supported by the National Natural Science Foundation of China (11904362), the Strategic Priority Research Program of the Chinese Academy of Sciences (XDB20000000), the Science and Technology Project of Fujian Province (2020H0038, 2019H0052), and the Youth Innovation Promotion Association of the Chinese Academy of Sciences.

References

1 E. Sun and W. Cao, *Prog. Mater. Sci.*, 2014, **65**, 124–210.
2 S. Zhang, F. Li, X. Jiang, J. Kim, J. Luo and X. Geng, *Prog. Mater. Sci.*, 2015, **68**, 1–66.
3 S. Zhang and F. Li, *J. Appl. Phys.*, 2012, **111**, 031301.
4 Z. Q. Duan, G. S. Xu, X. F. Wang, D. F. Yang, X. M. Pan and P. C. Wang, *Solid State Commun.*, 2005, **134**, 559–563.
5 C. He, X. Li, Z. Wang, Y. Liu, D. Shen, T. Li and X. Long, *J. Alloys Compd.*, 2012, **539**, 17–20.
6 X. Li, Z. Wang, C. He, Y. Liu, X. Long, S. Han and S. Pan, *Mater. Lett.*, 2015, **143**, 88–90.
7 C. Luo, W.-Y. Chang, M. Gao, C.-H. Chang, J. Li, D. Viehland, J. Tian and X. Jiang, *Acta Mater.*, 2020, **182**, 10–17.
8 C. He, T. Karaki, X. Yang, Y. Yamashita, Y. Sun and X. Long, *Jpn. J. Appl. Phys.*, 2019, **58**, SLLD06.
9 S. Wada and T. Tsurumi, *Br. Ceram. Trans.*, 2004, **103**, 93–96.
10 R. Ahluwalia, T. Lookman, A. Saxena and W. W. Cao, *Phys. Rev. B: Condens. Matter Mater. Phys.*, 2005, **72**, 014112.
11 D. Lin, S. Zhang, Z. Li, F. Li, Z. Xu, S. Wada, J. Luo and T. R. Shrout, *J. Appl. Phys.*, 2011, **110**, 084110.
12 Z. Yuan, S. Sang, E. Sun, X. Qi, W.-Y. Chang, R. Zhang, B. Yang, X. Jiang and W. Cao, *Crystengcomm*, 2018, **20**, 4745–4751.
13 F. Li, L. Wang, L. Jin, D. Lin, J. Li, Z. Li, Z. Xu and S. Zhang, *IEEE Trans. Ultrason. Ferroelectrics Freq. Contr.*, 2015, **62**, 18–32.
14 F. Li, M. J. Cabral, B. Xu, Z. Cheng, E. C. Dickey, J. M. LeBeau, J. Wang, J. Luo, S. Taylor, W. Hackenberger, L. Bellaiche, Z. Xu, L.-Q. Chen, T. R. Shrout and S. Zhang, *Science*, 2019, **364**, 264–268.
15 M. Gao, C. Luo, W.-Y. Chang, C. M. Leung, J. Tian, J. Li, X. Jiang and D. Viehland, *Acta Mater.*, 2019, **169**, 28–35.
16 M. Davis, M. Budimir, D. Damjanovic and N. Setter, *J. Appl. Phys.*, 2007, **101**, 054112.

17 F. Li, D. Lin, Z. Chen, Z. Cheng, J. Wang, C. Li, Z. Xu, Q. Huang, X. Liao, L.-Q. Chen, T. R. Shrout and S. Zhang, *Nat. Mater.*, 2018, **17**, 349–354.
18 F. Li, S. Zhang, Z. Xu, X. Wei and T. R. Shrout, *Adv. Funct. Mater.*, 2011, **21**, 2118–2128.
19 S. E. Park and T. R. Shrout, *IEEE Trans. Ultrason. Ferroelectrics Freq. Contr.*, 1997, **44**, 1140–1147.
20 Y. Yamashita, N. Yamamoto, Y. Hosono, K. Itsumi, *US Pat.*, 20150372219, 2015.
21 W.-Y. Chang, C.-C. Chung, C. Luo, T. Kim, Y. Yamashita, J. L. Jones and X. Jiang, *Mater. Res. Lett.*, 2018, **6**, 537–544.
22 J. Xu, H. Deng, Z. Zeng, Z. Zhang, K. Zhao, J. Chen, N. Nakamori, F. Wang, J. Ma, X. Li and H. Luo, *Appl. Phys. Lett.*, 2018, **112**, 182901.
23 C. Qiu, J. Liu, F. Li and Z. Xua, *J. Appl. Phys.*, 2019, **125**, 014102.
24 C. Qiu, B. Wang, N. Zhang, S. Zhang, J. Liu, D. Walker, Y. Wang, H. Tian, T. R. Shrout, Z. Xu, L.-Q. Chen and F. Li, *Nature*, 2020, **577**, 350–354.
25 F. Fang, W. Yang and X. Luo, *J. Appl. Phys.*, 2009, **106**, 094107.
26 F. Fang, X. Luo and W. Yang, *J. Am. Ceram. Soc.*, 2013, **96**, 228–233.
27 M. Shanthi, K. H. Hoe, C. Y. H. Lim and L. C. Lim, *Appl. Phys. Lett.*, 2005, **86**, 262908.
28 C. Luo, H. Wan, W.-Y. Chang, Y. Yamashita, A. R. Paterson, J. Jones and X. Jiang, *Appl. Phys. Lett.*, 2019, **115**, 192904.
29 J. Liu, C. Qiu, L. Qiao, K. Song, H. Guo, Z. Xu and F. Li, *J. Appl. Phys.*, 2020, **128**, 094104.
30 C. Luo, T. Karaki, Y. Sun, Y. Yamashita and J. Xu, *Jpn. J. Appl. Phys.*, 2020, **59**, SPPD07.
31 Y. Sun, T. Karaki, T. Fujii and Y. Yamashita, *Jpn. J. Appl. Phys.*, 2019, **58**, SLLC06.
32 M. Ma, S. Xia, K. Song, H. Guo, S. Fan and Z. Li, *J. Appl. Phys.*, 2020, **127**, 064106.
33 Z. Chen, Y. Zhang, S. Li, X.-M. Lu and W. Cao, *Appl. Phys. Lett.*, 2017, **110**, 202904.
34 F. Li, S. Zhang, Z. Xu, X. Wei, J. Luo and T. R. Shrout, *J. Appl. Phys.*, 2010, **108**, 034106.
35 L. Yang, H. Fang, L. Zheng, J. Du, L. Wang, X. Lu, W. Lu, R. Zhang and W. Cao, *Appl. Phys. Lett.*, 2019, **114**, 232901.
36 X. Huo, R. Zhang, L. Zheng, S. Zhang, R. Wang, J. Wang, S. Sang, B. Yang and W. Cao, *J. Am. Ceram. Soc.*, 2015, **98**, 1829–1835.
37 Q. Guo, F. Li, F. Xia, X. Gao, P. Wang, H. Hao, R. Sun, H. Liu and S. Zhang, *ACS Appl. Mater. Interfaces*, 2019, **11**, 43359–43367.
38 R. E. Eitel, T. R. Shrout and C. A. Randall, *J. Appl. Phys.*, 2006, **99**, 124110.
39 J. E. Garcia, R. Perez, D. A. Ochoa, A. Albareda, M. H. Lente and J. A. Eiras, *J. Appl. Phys.*, 2008, **103**, 054108.
40 H. Fang, L. Wang, W. Kuai, J. Du, G. Jiang, X. Lu, M. Zhao, C. Wang, W. Su, L. Zheng, C. Wang and C. Wang, *J. Am. Ceram. Soc.*, 2020, **103**, 3257–3264.
41 M. Davis, D. Damjanovic and N. Setter, *J. Appl. Phys.*, 2006, **100**, 084103.